Geoderma 431 (2023) 116375

Contents lists available at ScienceDirect

Geoderma

journal homepage: www.elsevier.com/locate/geoderma

Decreased CH_4 emissions associated with methanogenic and methanotrophic communities and their interactions following Fe(III) fertiliser application in rice paddies

Yihe Zhang [a], Mengyuan Huang [a], Kai Yu [a], Yuxin Xie [a], Yuxin Wang [a], Jie Wu [a], Fengwei Zheng [a], Shuang Wu [a,b], Shuqing Li [a,b,*], Jordi Sardans [c,d], Josep Peñuelas [c,d], Jianwen Zou [a,b]

[a] Jiangsu Key Laboratory of Low Carbon Agriculture and GHGs Mitigation, College of Resources and Environmental Sciences, Nanjing Agricultural University, Nanjing 210095, China
[b] Jiangsu Key Lab and Engineering Center for Solid Organic Waste Utilization, Jiangsu Collaborative Innovation Center for Solid Organic Waste Resource Utilization, Nanjing Agricultural University, Nanjing 210095, China
[c] CSIC, Global Ecology Unit CREAF-CSIC-UAB, Cerdanyola del Valles, Catalonia 08193, Spain
[d] CREAF, Cerdanyola del Valles, Catalonia 08193, Spain

ARTICLE INFO

Handling Editor: Diego Abalos

Keywords:
Fe(III) fertilisation
CH_4 emission
Rice paddies
Methanogens
Methanotrophs
Co-occurrence networks

ABSTRACT

Rice paddies are important sources of atmospheric methane (CH_4), where CH_4 fluxes are determined by the balance of production and oxidation. While the application of Fe(III) fertilizer is a proven effective strategy for mitigating CH_4 emissions from rice paddies, little is known about the role of methanogen and methanotroph communities and their interactions. In this study, we measured the CH_4 flux in a rice paddy field experiment, where the responses of methanogenic and methanotrophic activities to Fe(III) fertiliser applied at medium (Fe-M) and high (Fe-H) levels were examined using real-time quantitative PCR coupled with co-occurrence network analysis after Illumina MiSeq sequencing of the *mcrA* and *pmoA* genes. Relative to the control without Fe(III) fertiliser application, in the Fe-M and Fe-H treatments, seasonal CH_4 emissions were significantly decreased by 65% and 62%, respectively. Fe(III) fertilisation significantly decreased the copy numbers and potential activity of methanogens, and had an opposite effect on methanotrophs. We found *Methanothrix* was the predominant genus more adaptive to grow in Fe-rich environments. Fe(III) fertilisation caused a shift in the methanotrophic community towards a predominance of Type II methanotrophs. Soil total Fe concentration, soil electrical conductivity, and different valences of iron were key factors in the composition of methanogenic and methanotrophic communities. Fe(III) fertilisation led to a less complex community taxonomic structure mostly attributed to fewer nodes and edges in both the co-occurrence and mutual exclusion networks of methanogen and methanotrophs. Our findings suggest that adding Fe(III) fertiliser in rice paddies could mitigate CH_4 emissions by regulating both methanogens and methanotrophs.

1. Introduction

Methane (CH_4) is one of the most potent atmospheric greenhouse gases, with a 25-fold radiative forcing than carbon dioxide (CO_2) over a 100-year period (IPCC, 2013). In agriculture, CH_4 can be produced from fermentative digestion by ruminant livestock, stored manure, and waterlogging rice paddies. Estimated at 36 Tg yr^{-1} globally, CH_4 emissions from rice paddies are one of the most important anthropogenic sources of atmospheric CH_4 (IPCC, 2013).

Methane is mainly produced under anoxic conditions, where CH_4 fluxes depend on the combined performance of methanogenic and methanotrophic communities (Kong et al., 2019; Tokida et al., 2010; Wang et al., 2018). In the past decade, many studies have been dedicated to optimising agricultural practices for mitigating CH_4 emissions from rice paddies, such as crop residue incorporation, fertilisers and water regimes (Kong et al., 2019; Qin et al., 2010; Zou et al., 2004). In addition, it has been shown that a functional heavy metal-antagonist such as fertilisation with Fe(III) has the potential to mitigate CH_4

* Corresponding author at: Jiangsu Key Laboratory of Low Carbon Agriculture and GHGs Mitigation, College of Resources and Environmental Sciences, Nanjing Agricultural University, Nanjing 210095, China.
E-mail address: shuqingli@njau.edu.cn (S. Li).

https://doi.org/10.1016/j.geoderma.2023.116375
Received 5 July 2022; Received in revised form 1 February 2023; Accepted 3 February 2023
Available online 11 February 2023
0016-7061/© 2023 The Author(s). Published by Elsevier B.V. This is an open access article under the CC BY-NC-ND license (http://creativecommons.org/licenses/by-nc-nd/4.0/).

emissions from rice paddies (Chen et al., 2017). Fertilisers containing active Fe and Fe^{3+}, which can act as electron acceptors, have been shown to decrease CH_4 emissions from rice paddies (Ali et al., 2008; Arao et al., 2009; Gwon et al., 2018). Waterlogging can create an anoxic soil environment to favour Fe reduction coupled with organic matter mineralization, which can reduce the transfer of electrons by methanogenesis and eventually decrease CH_4 emissions (Fredrickson and Gorby, 1996; Lovley and Phillips, 1987; Sun et al., 2016). Moreover, CH_4 production can be suppressed by controlling the ratio of easily oxidizable organic matter to easily reducible iron. It is well documented that methanogenic archaea can be affected by Fe(III) fertiliser application in paddy soils. For example, Fe(III) in oxides or available Fe(III) may serve as an electron acceptor to suppress the growth of methanogens and thus influence the methane cycle (Bond and Lovley, 2002; Bowman et al., 1994; Lovley and Phillips, 1987). The inhibition of methanogenesis has been attributed to the competition between dissimilatory iron-reducing bacteria and methanogens (i.e., *Methanocella* and *Methanosarcina*) for the same substrate, such as hydrogen (Bodegom and Stams, 1999; Lovley, 1987).

On the other hand, aerobic interfaces of methanogenic environments may provide habitats for methanotrophs in rice paddies, where CH_4 can be oxidized by methanotrophs. While the studies of Fe(III) fertiliser effects on CH_4 emissions have mostly focused on the CH_4 production process driven by methanogens in rice paddies (Chen et al., 2017; Zhang et al., 2012), CH_4 oxidation, as an important link in the methane cycle, has attracted little attention in the context of Fe(III) fertiliser application in rice paddies. The distribution of Type I (*Gammaproteobacteria*) and Type II (*Alphaproteobacteria*) methanotrophs is highly related to soil physical and chemical properties, such as soil pH and salinisation, which need to be further examined following Fe(III) fertiliser application in rice paddies (Hanson and Hanson, 1996; Heyer et al., 2002; Ho et al., 2011). Therefore, qPCR and Illumina MiSeq sequencing techniques would provide an opportunity to simultaneously examine the abundance and community composition of methanogens and methanotrophs (Zhou et al., 2020), which would be helpful to gain insight into methane production and oxidation processes following Fe(III) fertiliser application in rice paddies.

Microorganisms can interact in complex communities that affect microbial processes in the environment (Kaupper et al., 2021). Recently, co-occurrence networks have been used to map all the relationships between microorganisms within a community, and these interactions can be divided into three categories: joint evolution of organisms in the environment (positive relationship known as co-occurrence); opposite evolution (negative relationship known as co-exclusion), and the absence of a relationship (a true lack of interaction or a null combination of all interactions between microorganisms) (Gross, 2008; Karimi et al., 2017). Network analysis has been widely adopted to investigate the co-occurrence patterns of methanogens and methanotrophs in soils (e.g., Fan et al., 2021; Kaupper et al., 2021). Specifically, the interaction network in the methanotrophic community became more complex during recovery from desiccation-rewetting, and active anaerobic oxidation of methane (AOM) pathways compensated a fraction of CH_4 produced during ongoing methanogenesis as identified by the network analysis (Kaupper et al., 2021; Fan et al., 2021). However, there is limited knowledge about how Fe(III) fertilisation impacts methanogenic and methanotrophic groups involved in commonly co-occurring links between networks.

To bridge this knowledge gap, we carried out a field experiment in the 2019 rice-growing season under different application levels of Fe(III) fertiliser. We measured the CH_4 fluxes, methane production potential (MPP), and methane oxidation potential (MOP) following Fe(III) fertiliser application in rice paddies. The abundance and diversity of the methanogens and methanotrophs were analysed by real-time quantitative PCR (qPCR) and Illumina MiSeq sequencing techniques, respectively. Community network analysis was adopted to describe the specific functional composition of methanogens and methanotrophs. We hypothesized that the response of CH_4 emissions to Fe(III) can be explained by the combined performance of methanogenic and methanotrophic communities (i.e., abundance, composition, and activity). The main objective of this study is to examine the Fe(III) fertiliser-induced decrease in CH_4 emissions associated with CH_4 production and oxidation processes in terms of the abundance and community structure of methanogens and methanotrophs.

2. Materials and methods

2.1. Site description and field experiments

The field experiment over the 2019 rice-growing season was conducted in a paddy field on an ecological landscape in Xinghua city, Jiangsu province, China (32°96′N, 120°01′E). In this rice paddy, Fe(III) fertiliser had not been applied before the experiment. The cropping regime of the experimental site was dominated by an annual paddy rice-winter wheat rotation system. The site has a typical monsoonal climate, with an average annual rainfall of 1049 mm and annual mean temperature of 14.8°C. The soil of the experimental site is classified as gleyic stagnic anthrosol, with a fine-scale soil texture (35.6% clay, 31.7% silt, 32.7% sand), a bulk density of 1.09 g cm^{-3}, a pH of 7.15 to 7.26, and a total nitrogen content of 1.15 g N kg^{-1}.

All experimental plots were managed in line with typical local cultivation practices (e.g., rice cultivar selection, tillage, water irrigation, nitrogen phosphorus and potassium fertiliser application regimes, and pest and weed control methods). The Fe(III) fertiliser used in this study was generally Fe(III) oxide-hydroxide hydrate, and the available iron content was 85%. The experimental treatment included Fe(III) fertiliser applied at three levels, namely, the control plots without Fe(III) fertiliser application and ferric hydroxide fertiliser($Fe(OH)_3$) applied at rates of 4.0 t ha^{-1} (Fe-M) and 8.0 t ha^{-1} (Fe-H). A random block design was adopted for the experimental plots with three replicates. Each field plot was 4 m by 4 m in size. In accordance with the local fertiliser regime, two chemical N fertiliser, namely, compound N fertiliser (N:P_2O_5:K_2O) and urea (46% N), were applied at a rate of 292 kg N ha^{-1} per plot, with 20% of the fertiliser applied as the base dose and the remaining 80% applied as topdressing at three time points over the rice-growing season. Basal fertiliser was spread and then mixed with the soil by ploughing on June 16, 2019.

The average active and free iron concentrations ranged between 52% and 60%; Fe(III) fertiliser application rates in the Fe-M and Fe-H treatments represent the local recommended medium and high levels for rice cultivation in Southeast China, respectively (Zhou et al., 2009). All plots were flooded two days prior to rice sowing (15 June 2019) and remained flooded until 29 August 2019; thereafter, the plots were drained and remained in the drainage stage until crop harvest. The cropping period (from planting to harvest) was roughly June-September for the 2019 rice-growing season. In the Fe(III)-fertilised plots, Fe(III) fertiliser together with crop residue was incorporated at a soil depth of 10–15 cm before flooding was initiated. Fe(III) fertiliser and crop residue were adequately mechanically mixed prior to incorporation.

2.2. Gas sampling and flux measurement

The fluxes of CH_4 were measured in situ using the static chamber-gas chromatograph (GC) method detailed in Kong et al. (2019). Before the fields were initially flooded, specially made aluminium flux collars (0.4 m long by 0.4 m wide by 0.15 m tall) were permanently installed in each field plot to ensure the reproducible placement of the gas-collecting chambers for gas sampling over the rice-growing season. The top edge of the collar had a groove that was filled with water to seal the rim of the chamber. The sampling chambers were made of opaque PVC materials and were 0.4 m long by 0.4 m wide by 0.5 m tall. The chamber inside was equipped with a circulating fan to ensure complete gas mixing, and it was wrapped with a layer of sponge and aluminium foil to minimise

air temperature changes inside the chamber during the sampling period. For gas sampling, the rim of the chamber was placed into the groove of the collar, including any vegetation growth. Soil CH_4 fluxes were measured once a week before N fertiliser application and then three times a week. Gas samples were collected at 0, 5, 10, 15, and 20 min after chamber closure between 09:00 and 11:00 LST on each sampling day. Individual gas samples of 60 mL were collected from the headspace of the chamber using gas sampling bags and then transported to the laboratory for analysis by GC within a few hours.

The gas samples were analysed using a modified GC (Agilent 7890A) equipped with a flame ionisation detector (FID) (Qin et al., 2010; Zou et al., 2009). The oven and FID were operated at 55°C and 200°C, respectively. The carrier gas (N_2) flow rate was 30 mL min^{-1}. A nonlinear fitting approach based on the slope of the change in the mixing ratio over time (measured at 0, 5, 10, 15, and 20 min) was applied to determine the CH_4 flux. The average and standard deviations of the CH_4 flux for each treatment were calculated from three replicates. Seasonal total CH_4 emissions were determined as the sequential accumulation of the flux measurements between every-two adjacent temporal intervals (Zou et al., 2005). Yield-scaled CH_4 emissions were calculated as the seasonal total of CH_4 emissions divided by rice yield for each plot.

2.3. Measurement of methane production and oxidation potentials

In each experimental plot, rhizosphere soil samples (0–20 cm) were collected on 14 August 2019 and 2 October 2019 to investigate the effects of Fe(III) fertiliser on methane production potential (MPP) and methane oxidation potential (MOP) during the waterlogging and drainage stages. The 10 g soil samples used to measure the MPP and MOP were homogenized before being placed into bottles. The MPP was determined according to the method described by Singh et al. (2012) with minor modifications. Briefly, 10 mL of anoxic sterile water was added to 10 g of fresh soil samples in a 100 mL serum bottle to ensure the soil was covered by a 10 mm water. To create an anaerobic environment, we repeatedly purged the headspace of serum bottles with O_2-free N_2 gas for 3 min to remove residual CH_4 and O_2, before incubating them in a dark environment at 30 °C for approximately 72 h. Before gas sampling, the serum bottles were shaken vigorously to establish equilibrium between the liquid and gas phases. Then, gas samples (4 mL) were collected from the headspace with a 5 mL syringe, and an equal volume of N_2 was injected back into the bottle afterwards. Gas samples were taken at intervals of 1, 60, and 120 h. Then, the gas samples were analysed for CH_4 using a gas chromatograph.

The methane oxidation potential (MOP) was determined by adding 10 g of soil and 10 mL of deionized water into a 150 mL serum bottle, according to the method described in Gao et al. (2020) and Kim et al. (2016). Approximately 1.5 mL of CH_4 (10 000 ppmv) was injected into each bottle using a 10 mL syringe and then dark-incubated and shaken at 120 rpm at 30 °C for two days. Gas samples (4 mL) were collected as described above, and an equal volume of air was injected back into the bottles after each gas sampling. The concentration of CH_4 was measured every 2 h on the first day and every 3 h on the second day, as in Gao et al (2020). The MPP or MOP was calculated by the following formula:

MPP or MOP ($\mu g\ g^{-1}\ d^{-1}$) $= \frac{K \times V}{W \times (1 - WH/100)}$, where K ($\mu g\ g^{-1}\ d^{-1}$) is the slope of the linear curve for the accumulated CH_4 concentration determined over an interval of three sampling times; V (L) is the volume of the serum bottle; W (g) is the weight of fresh soil; and WH (g) is the weight of H_2O per 100 g fresh soil.

2.4. Soil sampling and analysis

Before rice sowing, soil samples from three replicate plots were collected and mixed thoroughly to measure the soil physicochemical properties. In addition, soil samples were collected once a week before N fertilisation and then twice or three times a week to examine seasonal variations in soil properties (Table S1). Soil samples were collected from the plough layer (0–20 cm) for each of the three replicates per treatment. All rhizosphere soil was gently scraped from the roots before placing the soil into a sterile sealable plastic bag, which was transported to the laboratory in an ice box containing liquid nitrogen. The fresh soil samples stored at 4°C were used to analyze soil physicochemical properties after undergoing air drying at 25°C within one week of sampling. The rest of the rhizosphere soil samples were stored at −80°C to determine microbial indicators. Prior to analysis, all soil subsamples were ground to pass through a 2 mm sieve. The contents of soil NO_3^--N and NH_4^+-N were measured using continuous flow analysis (Skalar SANplus analyser, Amsterdam, Netherlands). The methods we used for determining soil physicochemical properties (pH, EC, TC, TN, C/N, and dissolved organic carbon, or DOC) are described in Kong et al. (2019) and Yu et al. (2021). The total Fe concentration was measured by digestion with HF-HNO_3-H_2O_2. The content of soil Fe^{2+} was measured using the ferrozine-ultraviolet absorbance method (Stookey, 1970). Grain yield was measured at the physiological maturity stage by hand-harvesting all plants in each 4 m × 4 m plot. Above-ground biomass, including rice straw and grain yield, was measured at harvest time by oven drying the samples at approximately 75°C to a constant weight.

2.5. DNA extraction and real-time PCR assays

Total genomic DNA samples were extracted using MO BIO PowerSoil DNA Isolation Kits (MO BIO Laboratories, Carlsbad, CA, USA) according to the manufacturer's instructions. The concentration of DNA samples was determined by Nanodrop (Thermo Scientific, USA). Then, DNA samples were used for quantitative polymerase chain reaction (qPCR) and Illumina MiSeq sequencing analysis.

The copy numbers of the *mcrA* and *pmoA* genes were determined in a StepOne™ real-time PCR system (Applied Biosystems, Germany) using the primer pair mlas/mcrA-rev (Steinberg and Regan, 2008) and A189F/Mb661R (Costello and Lidstrom, 1999), respectively. The qPCR amplifications were performed in a total volume of 20 μL using SYBR® Premix Ex Taq (Takara, China) with a reaction mixture of 10 μL of SYBR® Premix Ex Taq™, 0.4 μL of each primer (10 μmol/L), 0.4 μL of ROX reference dye (50 ×), 2 μL of template DNA and 6.8 μL of sterile water. The amplified fragments for each gene were cloned in the pMD 18-T vector and sequenced. The standard curves for both genes were prepared by using triplicate 10-fold dilutions of linear plasmid DNA. Amplification was performed in triplicate under the following cycling conditions: 30 s at 95 °C; 40 cycles at 95 °C, 55 °C and 72 °C for 5 s, 30 s, and 15 s, respectively; and a dissociation stage at 95 °C for 15 s, 55 °C for 30 s, and 95 °C for 15 s (Li et al., 2017).

2.6. Illumina MiSeq sequencing

The structures of the methanogen and methanotroph communities were assessed by Illumina MiSeq sequencing of the *mcrA* and *pmoA* genes, respectively. The highly conserved *mcrA* gene encoding the α-subunit of methyl coenzyme M reductase has been widely used for analysis and quantification of methanogen communities, and the *pmoA* gene encoding methane monooxygenase subunit A is used as the indicator for quantifying the methanotrophs from environmental samples (Pereyra et al., 2010; Sonoki et al., 2013; Wasmund et al., 2009). The mlas/*mcrA*-rev (Steinberg and Regan, 2008) and A189F/Mb661R (Holmes et al., 1995) primers were set up for amplification of the *mcrA* and *pmoA* genes, respectively. The Axyprep DNA Gel Extraction Kit (Axygen Biosciences, Union City, CA, USA) was used to purify the targeted bands (approximately 410 bp for *mcrA* and 478 bp for *pmoA*), and QuantiFluor™-ST (Promega, Madison, WI, USA) was employed to quantify the targeted bands. For each sample, PCR was repeated in triplicate, prior to mixing the three PCR products. The PCR products of each DNA sample were evaluated by 2% agarose gel electrophoresis. The

equimolar purified amplicons were pooled and paired-end sequenced (2 × 250) on the Illumina MiSeq platform according to the standard protocols at Shanghai BIOZERON Biotechnology Co., ltd. (Shanghai, China). The Illumina MiSeq sequencing data are available in the NCBI Sequence Read Archive (SRA) database under accession number PRJNA725635.

2.7. Illumina data analysis

According to Caporaso et al. (2010), we found three criteria for demultiplexing and quantity filtering the raw *mcrA* and *pmoA* sequences by Quantitative Insights Into Microbial Ecology (QIIME) (Version 1.17) after sequencing was completed: (1) sequences with reads shorter than 200 bp and quantity scores below 25 were discarded from further analysis; (2) sequences were clustered into operational taxonomy units (OTUs) at a 97% identity threshold; and (3) UCHIME was used to identify and remove chimeric sequences (Edgar et al., 2011). The *mcrA* sequences were binned into species-level OTUs at 84% sequence identity, corresponding to 97% similarity based on the 16S rRNA gene by using UCLUST (Yang et al., 2014), and *pmoA* sequences that shared 87% similarity, corresponding to 97% similarity based on the 16S rRNA gene, were binned into species-level OTUs with UCLUST (Degelmann et al., 2010). The taxonomy of the *mcrA* and *pmoA* genes was analysed using the Non-Redundant Protein Sequence Database. To calculate the α-diversity of the methanogen community, we used the abundance-based coverage estimator (ACE), Chao1 estimator, Shannon diversity and Good's coverage.

2.8. Construction of the microbial co-occurrence network

Co-occurrence network analysis was performed based on the proportionally normalized OTU tables with Cytoscape (v3.8.2) software using the CoNet plug-in (v1.1.1). Prior to network construction, *mcrA* and *pmoA* relative abundance matrices were grouped into a single matrix so that links could be computed between OTUs of the same variant (i.e., pairs of *mcrA*-*mcrA* or *pmoA*-*pmoA*) and between OTUs of different variants (i.e., *mcrA*-*pmoA*). To reduce false-positive predictions, the taxa represented in above one-third of the samples were reserved for network analysis. Copresence and exclusion links were identified with an ensemble-based approach, including two measures of correlation (Pearson and Spearman) and dissimilarity (Bray-Curtis and Kullback-Leibler) to increase the robustness of the analysis (Faust and Raes, 2016). The interaction sign was used to distinguish between co-presence and exclusion links, which were considered undirected because of the nature of the correlation or dissimilarity measures used. Statistical significance was tested by obtaining the link- and measure-specific p value as the mean of the permutation distribution under the bootstrap distribution, using 1000 iterations for each distribution. Probability values for different correlation or dissimilarity measures supporting the same link were merged using Brown's method and corrected for multiple testing using the Benjamini–Hochberg procedure. Finally, to reduce the detection of false positives, we included only those links supported by at least two measures of correlation or dissimilarity and having an adjusted merged p value below 0.05. The correlation results were then imported into Gephi (v0.9.2), and the microbial co-occurrence network was visualised using the Fruchterman Reingold algorithm. The network topological parameters, including the degree of each node, clustering coefficient, network density and average path distance were calculated in Gephi (v0.9.2).

2.9. Statistical analysis

Two-way analysis of variance (ANOVA) was used to examine the main and interaction effects of Fe(III) fertiliser treatment and flooding or drainage stages on the abundance and activity of methanogens and methanotrophs. The correlations of CH_4 fluxes with methanogenic and methanotrophic abundance and activities were fitted by a linear model with ordinary least squares (OLS). A t test was used to examine the statistical significance of parameter estimates in the simulated OLS model. Spearman correlation coefficients were employed to test the relationships between soil properties and the relative abundance of genera in R. Statistical significance was determined at the 0.05 probability level. A permutational multivariate analysis of variance (PERMANOVA) was conducted using the Adonis function in the R vegan package with 999 permutations to test the significance of independent variables that accounted for the divergence in communities of methanogens and methanotrophs (standard Mantel test). Redundancy analysis (RDA) of OTUs was performed to summarize the variations in methanogenic and methanotrophic communities that could be explained by the soil properties using the ggbiplot package in R. The means of different relative abundance of methanogenic genera from The Fe(III) fertilised treatment (X_e) and control (X_a) groups were used to evaluate effect size in the form of the natural log-transformed response ratio (ln$R$). The standard deviations of both treatment and control groups were included as a measure of variance:

$$\ln R = \ln\left(\frac{Xe}{Xa}\right)$$

where X_e and X_a are means in the Fe(III) fertilised treatment and control groups, respectively. The mean response ratio (RR_{++}) is calculated from the individual lnR of each paired comparison between control and treatment groups with the weight of each lnR using a categorical random effect model (Zheng et al., 2020). Fe-M and Fe-H treatments were merged to assess the effects of the methanogen community composition on the paddy soil. The effects of different methanogenic genera were considered significant if the 95% CI did not overlap with the line ln$R$ = 0.

3. Results

3.1. CH_4 fluxes

The seasonal pattern of CH_4 fluxes did not differ with Fe(III) fertiliser application while being sensitive to the water regime (Fig. 1). During initial flooding the CH_4 fluxes remained at low levels within 35 days of broadcast sowing. Thereafter, the CH_4 fluxes increased to the largest values in the following two–three weeks. The CH_4 fluxes rapidly decreased because of the midseason drainage episode, followed by relatively low flux rates until harvesting.

A two-way ANOVA indicated that CH_4 emissions were significantly affected by Fe(III) fertiliser, flooding or drainage episodes and their interaction (Table 1 and 2). The average seasonal CH_4 fluxes from the control plots were 33.33 mg m^{-2} day^{-1}, 186% and 166% greater than those from the Fe-M and Fe-H treatments, respectively. Substantial CH_4 emissions occurred mostly during flooding episodes for all treatments. Relative to the control, in the treatment, Fe(III) fertiliser application significantly decreased yield-scaled CH_4 emissions; these did not differ between the Fe-M and Fe-H treatments (Table 2).

3.2. Soil physicochemical properties

Fe(III) fertiliser application significantly increased soil EC and pH ($p < 0.05$) over the rice-growing season (Fig. S1). Soil NH_4^+-N showed a significant and positive relationship with CH_4 fluxes (Fig. S1 and Table S1). The concentrations of total Fe and Fe(II) in the soil were measured to gain insight into the transformation of Fe during two typical periods of rice growth (Fig. S2). Relative to the control, soil total Fe and Fe(II) concentrations were significantly greater in the Fe(III)-fertilised treatments in the flooding episode ($p < 0.05$). However, this difference was not pronounced in the late drainage stage of rice cultivation, suggesting there were unique anoxic conditions favourable for the

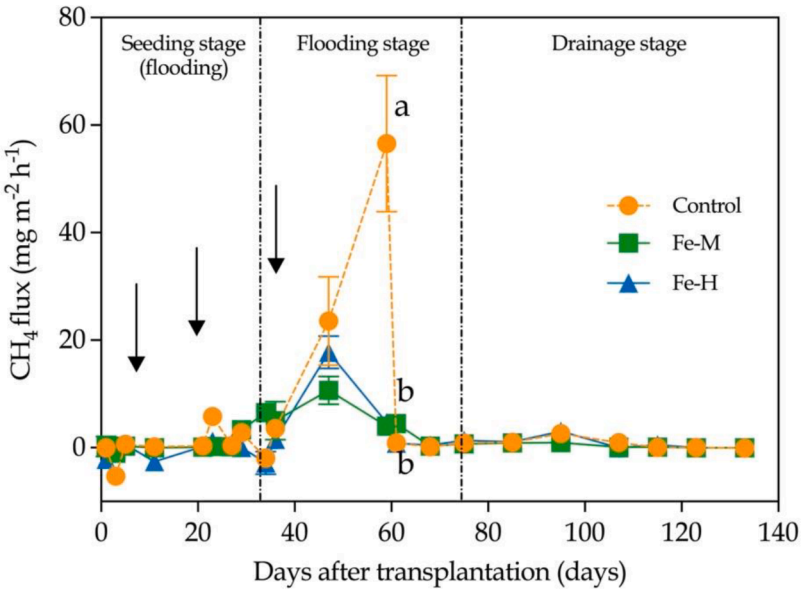

Fig. 1. Seasonal dynamics of CH_4 fluxes and cumulative CH_4 emissions as affected by different levels of Fe fertiliser in the 2019 rice season. The control group corresponds to no Fe(III) fertiliser addition; the Fe-M treatment corresponds to a medium concentration of Fe(III) fertiliser; the Fe-H treatment corresponds to a high concentration of Fe(III) fertiliser. Vertical bars indicate the standard errors of three replicates. Black arrows represent fertilisation time points. Letters *a* and *b* indicate significant differences at $p < 0.05$ level.

Table 1
Two-way analysis of variance (ANOVA) of methane production potential (MPP), methane oxidation potential (MOP), and log copy numbers of *mcrA* and *pmoA* genes; df: degree of freedom, MS: mean square, and *F*: *F* value. *, **, and *** denote $p < 0.05$, $p < 0.01$, and $p < 0.001$, respectively.

Source of variance	df	CH_4 fluxes		MPP		MOP		*mcrA*		*pmoA*	
		MS	*F*	MS	*F*	MS	*F*	MS	*F*	MS	*F*
Fe(III) fertiliser levels	2	1412.2	17.53***	66.181	44.124***	4.46×10^4	18.65***	0.812	21.745***	0.273	7.54**
Flooding/Drainage	1	2063.4	25.61***	23.029	15.354**	1.28×10^5	53.33***	0.486	13.008**	3.446	95.023***
Fe(III) fertiliser levels × Flooding/Drainage	2	1317.4	16.35***	12.545	8.364**	4.35×10^3	1.82	0.031	0.826	0.017	0.477

Table 2
Seasonal CH_4 emissions (kg ha^{-1}), grain yield (t/ha), and yield-scaled CH_4 (kg CH_4 t^{-1} yield) from rice paddies treated with different concentrations of Fe fertiliser regimes over the 2019 season. Control: no Fe fertiliser; Fe-M: medium concentration of Fe fertiliser; Fe-H: high concentration of Fe fertiliser. Different letters (*a, b*) indicate a significant difference between treatments at $p < 0.05$.

Treatments	Seasonal CH_4 emissions		Grain yield	Yield-scaled CH_4
	Flooding (kg ha^{-1})	Drainage (kg ha^{-1})	(t/ha)	(kg CH_4 t^{-1} yield)
Control	170.92 ± 22.32 a	12.68 ± 2.23 a	10.26 ± 0.62 a	18.24 ± 2.61 a
Fe-M	57.78 ± 6.90b	5.84 ± 0.77 a	10.39 ± 0.60 a	6.20 ± 0.36b
Fe-H	54.77 ± 3.29b	12.85 ± 2.03 a	10.03 ± 0.78 a	7.06 ± 1.07b

conversion between Fe^{3+} and Fe^{2+} in rice paddies.

3.3. Methane production potential (MPP) and methane oxidation potential (MOP)

A two-way ANOVA showed that the Fe(III) fertiliser and flooding or drainage episodes significantly altered the MPP and MOP, while their interaction, to a large extent, affected the MPP (Fig. 2 and Table 1). Relative to the control plots, the MPPs of the Fe-M and Fe-H treatments were significantly decreased by 60% and 72% during the flooding period and by 34% and 59% during the drainage period, respectively (Fig. 2a). In contrast, the MOPs were significantly greater in the Fe-M and Fe-H treatments than in the control ($p < 0.05$), suggesting that Fe(III) fertiliser application can facilitate soil CH_4 oxidation. Moreover, a significant positive correlation was found between the MPPs and CH_4 fluxes, in contrast to a negative correlation between the MOPs and CH_4 fluxes ($p < 0.01$; Fig. S3).

3.4. The response of methanogenic population size and community composition to Fe(III) fertilisation

Both methanogenic population size and community composition were significantly affected by Fe(III) fertiliser application. The *mcrA* absolute abundance is significantly lower, by 67% and 86%, respectively, in the Fe-M and Fe-H treatments than in the control ($p < 0.05$) (Fig. S4a). In the methanogenic community, the top eight most abundant methanogenic genera were identified. Together, they account for almost 85% of the relative abundance of all methanogenic groups. *Methanothrix* (15.03%-34.46%), *Methanocella* (17.97%-25.95%), and *Methanobacterium* (24.41%-29.17%) are the three most abundant genera (Fig. 3a). Fe(III) fertiliser application significantly altered the methanogenic community composition. Specifically, the relative abundance of *Methanothrix* increased by 77%, and that of *Methanocella* and *Methanobacterium* decreased by 32% (95% Cl, 37–22%) and 13%, respectively (Fig. 4a). Furthermore, both the Fe(III) fertiliser-increased and Fe (III) fertiliser-decreased genera were significantly related to CH_4 fluxes, but the regression line has a steeper slope (4.71) for the decreased genera than for the increased genera (2.79) (ANOVA, $p < 0.01$, Fig. 4b).

Redundancy analysis (RDA) and the standard Mantel test were used to investigate the relationship between the soil microbial composition of methanogens and methanotrophs (OTUs data) and soil properties. The RDA biplot revealed that 95% of the total variability is explained by the first two axes of the RDA (Fig. 5a). In general, the MPPs, NH_4^+-N, EC, total Fe and Fe^{2+} concentrations show a significant relationship with the methanogenic community ($p < 0.01$). The methanogenic communities in the Fe-M and Fe-H treatments are separated from those in the control along the x-axis of the RDA plots. In the Fe-M and Fe-H treatments, the

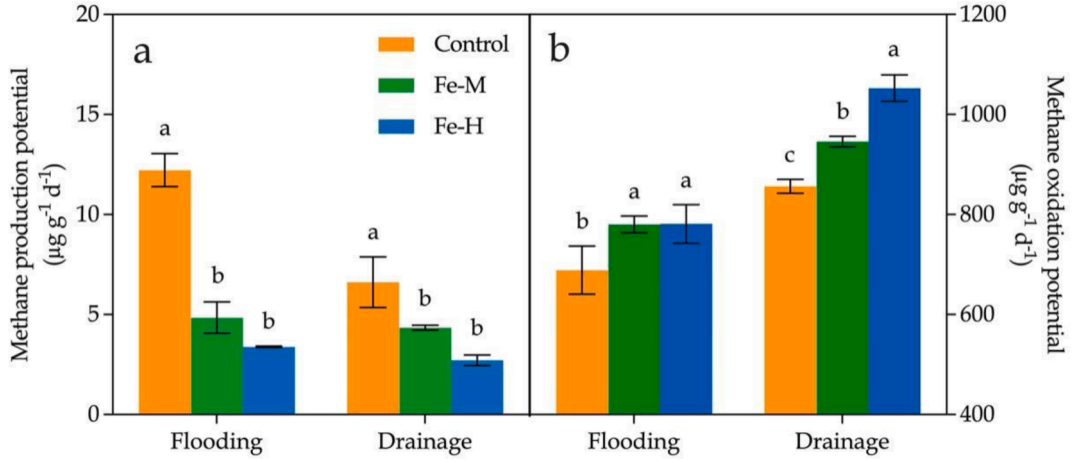

Fig. 2. Methane production potentials (a) and methane oxidation potentials (b) under different levels of Fe(III) fertilisation treatments. Values are means ± SE (n = 3). Different letters (a, b, c) indicate a significant difference between treatments at p value < 0.05.

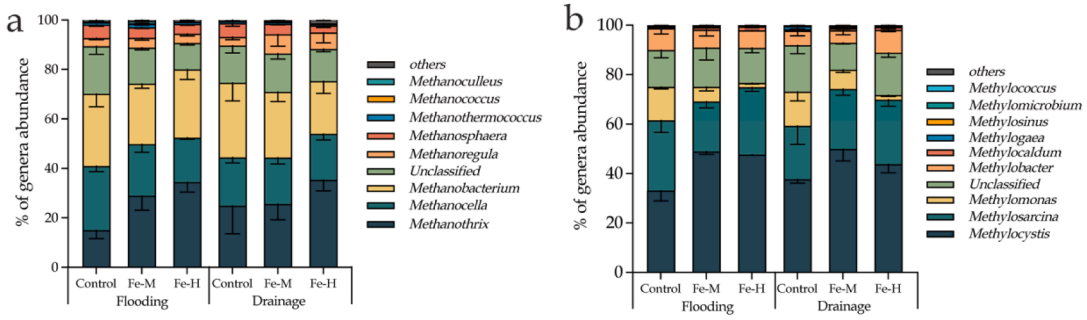

Fig. 3. Relative abundance of methanogens (a) and methanotrophs (b) under different levels of Fe(III) fertilisation treatments at different water management stages. Relative abundance of methanogens and methanotrophs for the taxonomic levels of the genus. Values are means ± SE (n = 3).

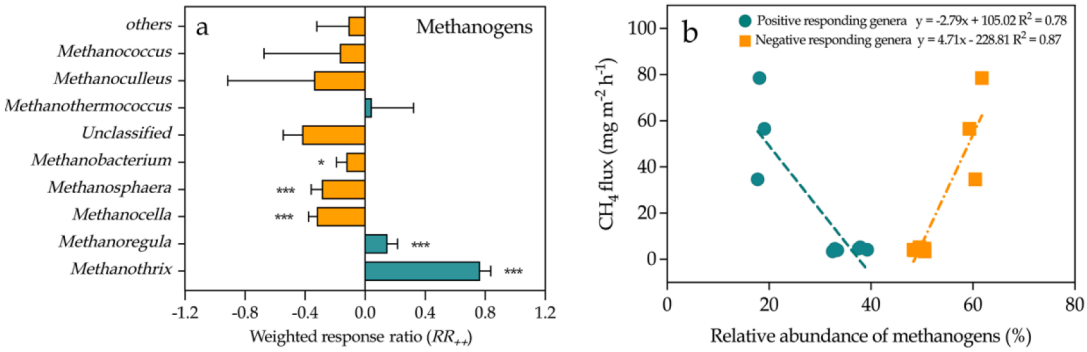

Fig. 4. (a) Top 8 most abundant methanogenic genera, other less abundant genera, and unclassified genera in response to Fe(III) fertiliser amendment during flooding episodes. Error bars represent 95% bias-corrected confidence intervals. Asterisks denote significant differences from the control plots (without Fe(III) fertiliser). * $p < 0.05$, ** $p < 0.01$, *** $p < 0.001$. (b) Dependence of CH_4 fluxes on the relative abundance of methanogenic genera that responded positively and negatively to treatment analysed from (a).

methanogenic composition is negatively related to MPPs but positively related to EC, total Fe, and Fe^{2+} concentration. Indeed, the dominant genera (*Methanothrix* and *Methanocella*) are both significantly related to the Fe(II) concentration, and MPPs ($p < 0.05$; Fig. 6a). Therefore, Fe(III) fertiliser application stimulated the electrovalence of Fe, leading to changes in methanogenic abundance and structure that affected CH_4 production potentials.

3.5. *The response of methanotrophic population and community compositions to Fe(III) fertilisation*

The results show a trade-off between the absolute abundances of *mcrA* and *pmoA* over the flooding and drainage episodes (Fig. S4). Fe(III) fertilisation had a positive effect on *pmoA* absolute abundance during flooding period and no significant effect difference during the drainage stage (Fig. S4b). A negative correlation ($R^2 = 0.68$, $p < 0.01$) was found between the CH_4 flux and *pmoA* absolute abundance across different levels of Fe(III) fertilisation over the rice-growing season (Fig. 6b).

The overall distribution pattern and α-diversity of the

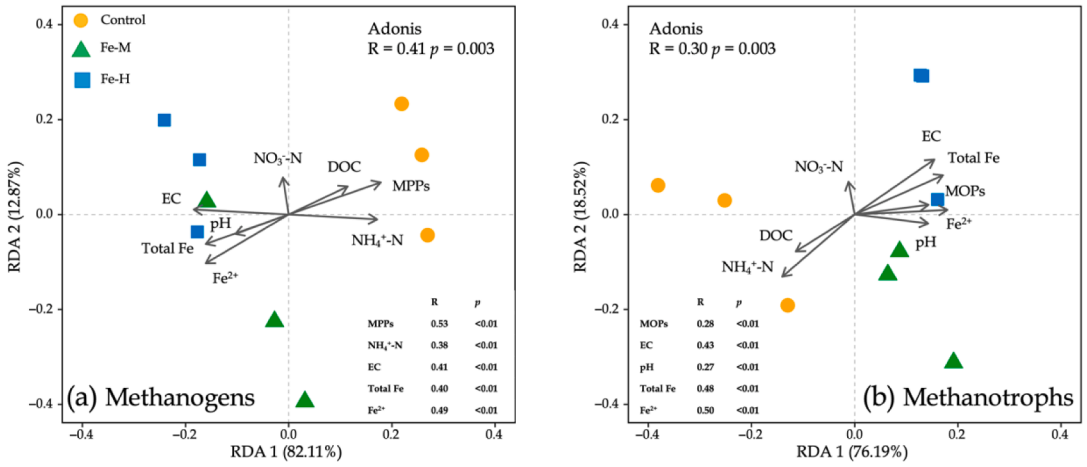

Fig. 5. Redundancy analysis (RDA) biplot of the relationship between methanogenic (a) and methanotrophic (b) communities and soil properties at the flooding stage over the 2019 rice-growing season. Treatments defined as in Fig. 1.

methanotrophic community at the genus level were not significantly affected by Fe(III) fertilisation, flooding or drainage episodes, or their interactions (Table S2). However, adding Fe(III) fertilisation altered the relative abundance of methanotrophic genera. The methanotroph community consisted of Type I genera, including *Methylosarcina*, *Methylomonas*, *Methylobacter*, *Methylocaldum*, *Methylogaea*, *Methylomicrobium* and *Methylococcus,* and Type II genera, including *Methylocystis* and *Methylococcus* (Fig. 3b). *Methylosarcina* and *Methylomonas* of Type I methanotrophs and *Methylocystis* of Type II methanotrophs were identified as the main methanotrophs, accounting for 72–82% of the total abundance. Fe(III)-fertilised plots were dominated by the *Methylocystis* genus in Type II methanotrophs (44–50%), which were more abundant than in the control (33%). In contrast, the relative abundance of *Methylomonas* (Type I methanotrophs) was lower in the treatments than in the control. Therefore, the application of Fe(III) fertiliser could have altered the methanotrophic community composition, mainly by increasing Type II methanotrophs (*Methylocystis* genus) and decreasing Type I methanotrophs (*Methylomonas* genus).

Unlike for methanogens, for methanotrophs, the three treatments are clustered on the redundancy analysis biplot (Fig. 5b). MOPs, EC, pH, total Fe and Fe^{2+} concentration show a significant relationship with methanotrophic composition ($p < 0.01$), and are especially positively correlated with Fe-M and Fe-H treatments. Furthermore, the pairwise correlation revealed that soil properties such as the EC and the electrovalence of Fe contributed most to the difference in key methanotrophic genera between treatments.

3.6. Microbial co-occurrence network

The integrated co-occurrence networks across methanogens and methanotrophs were compared between the control and Fe-H treatments in the flooding stage. The network of the control is more complex than that of the Fe-H treatment, consisting of more nodes and edges (97 nodes and 854 edges in the control vs 95 nodes and 741 edges in the Fe-H treatment) (Fig. 7, Table 3). In the control group, *Methanocella* and *Methylocystis* are the most dominant genera in the methanogenic and methanotrophic networks, respectively. However, in the Fe-H treatment, the proportion of *Methanothrix* is higher than that of the other genera (Tables S3 and S4). Relative to the control, the Fe-H treatment has a lower average path distance (2.167 vs 2.367 in the control), lower average degree (15.6 vs 17.608 in the control), lower clustering coefficient (0.518 vs 0.633 in the control) and lower network density (0.166 vs 0.183 in the control) (Table 3).

Additionally, the co-occurrence networks of methanogens and methanotrophs were also analysed (Fig. 7b). Although in both treatments the nodes are largely comparable, there are fewer network edges in the Fe-H treatment (for methanogens, 289 vs 329 in the control, and for methanotrophs, 130 vs 144 in the control) (Fig. 7b; Table 4). Moreover, the average degree, clustering coefficient, and network density in the Fe-H treatment are lower than those in the control (Table 4). The most obvious difference was observed in the methanogenic mutual exclusion networks (49 nodes and 47 edges vs 48 nodes and 109 edges in the control).

4. Discussion

In agreement with previous studies, our results show the rice grain yields were not significantly affected by Fe(III) fertiliser application (Table 2) (He et al., 2013; Xu et al., 2018). The effects of the two Fe(III) fertilisation treatments on CH_4 emissions in paddy soils are not significantly different, which can be explained by the absence of the difference in the concentration of soil total Fe and Fe^{2+}. The seasonal CH_4 emissions from the control totalled 184.73 kg CH_4 ha^{-1}, and Fe(III) fertiliser application significantly decreased the seasonal CH_4 emissions by 62–65%.

The mitigation of CH_4 emissions by Fe(III) fertiliser amendment could be attributed to changes in the abundance and composition of methanogen and methanotroph communities. Generally, iron oxides and their biological reduction processes directly or indirectly affect anaerobic methanogenesis and methane oxidation processes in an anoxic environment (Beal et al., 2009; Weber et al., 2006). The addition of Fe(III) fertiliser can promote the reduction of Fe(III) and lead to a decrease in methanogen abundance (Figs. S2a and S4a). This inhibition is primarily explained by the competition between methanogens and dissimilatory Fe(III)-reducing bacteria (DIRB) for the common substrates acetate and hydrogen, together with the direct inhibition of methanogenesis by amorphous $Fe(OH)_3$ at some concentrations (Van Bodegom et al., 2004). Recently, more attention has been paid to the anaerobic oxidation of methane (AOM) coupled with alternative electron acceptors (AEAs) because of its potential activity of consuming CH_4 in different environments, such as freshwater sediments (Beal et al., 2009), peatlands (Reumer et al., 2018), tropical soils (Blazewicz et al., 2012) and rice paddies (Fan et al., 2019). However, Fan et al. (2020) reported that adding Fe^{3+} did not support AOM and even partially suppressed the AOM rates. In this study, amendment with Fe(III) fertiliser (Fe-M and Fe-H) significantly stimulated the absolute abundance of aerobic methanotrophs during the flooding stage ($p < 0.05$) by about 62% and 68%, respectively. Moreover, we found soil salinity can induce an increase in *pmoA* gene abundance in the Fe(III) fertilised treatment, because different methanotrophic genera may show distinct degrees of

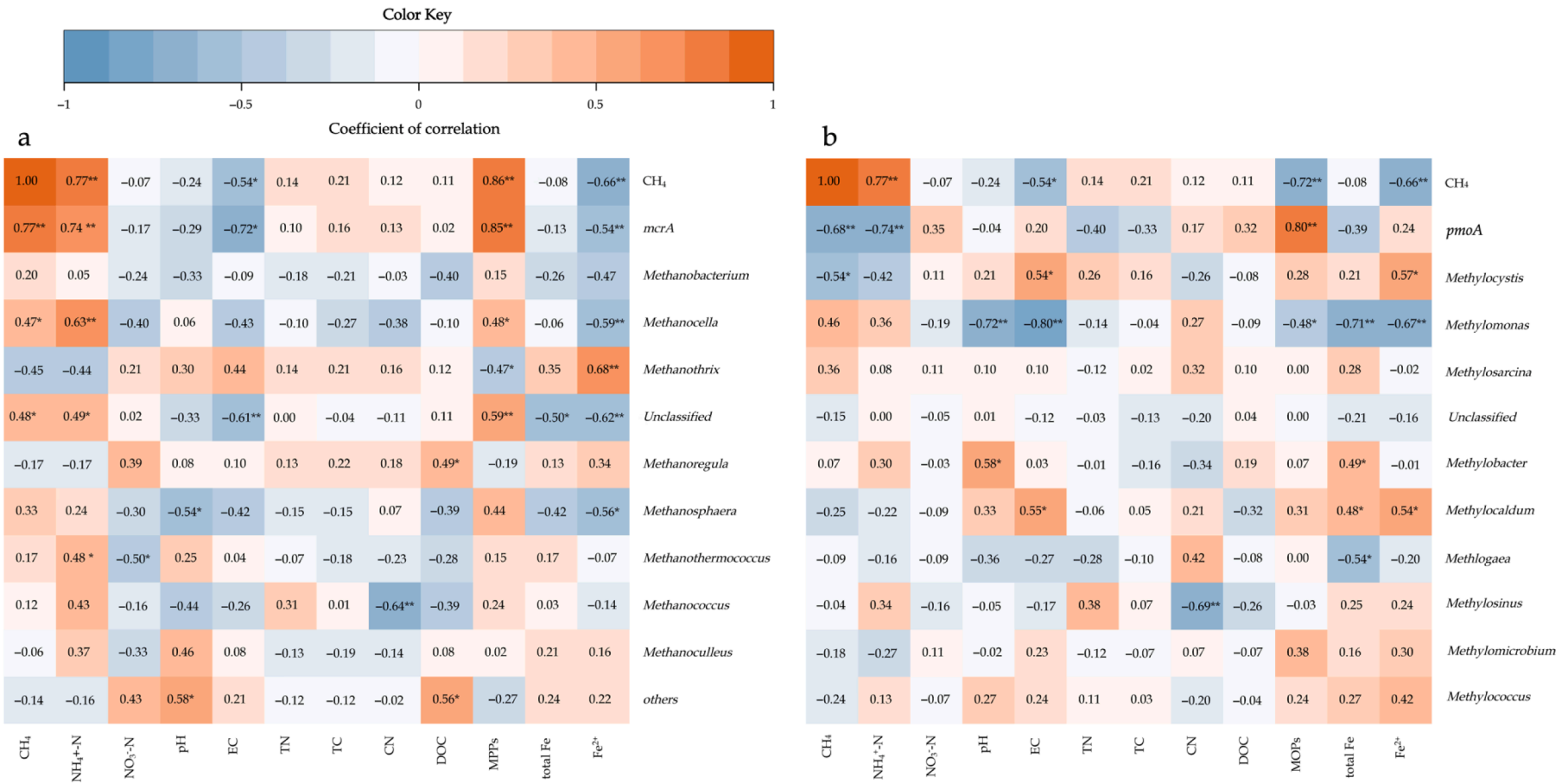

Fig. 6. Correlations between the CH_4 emissions, the relative abundance of dominant methanogens (a) and methanotrophs (b), and soil physicochemical properties in the rice paddy soil shown as coloured covariance matrices. From porcelain white to navy blue, darker boxes represent stronger correlation coefficients; lighter boxes represent lower correlations. * $p < 0.05$, ** $p < 0.01$.

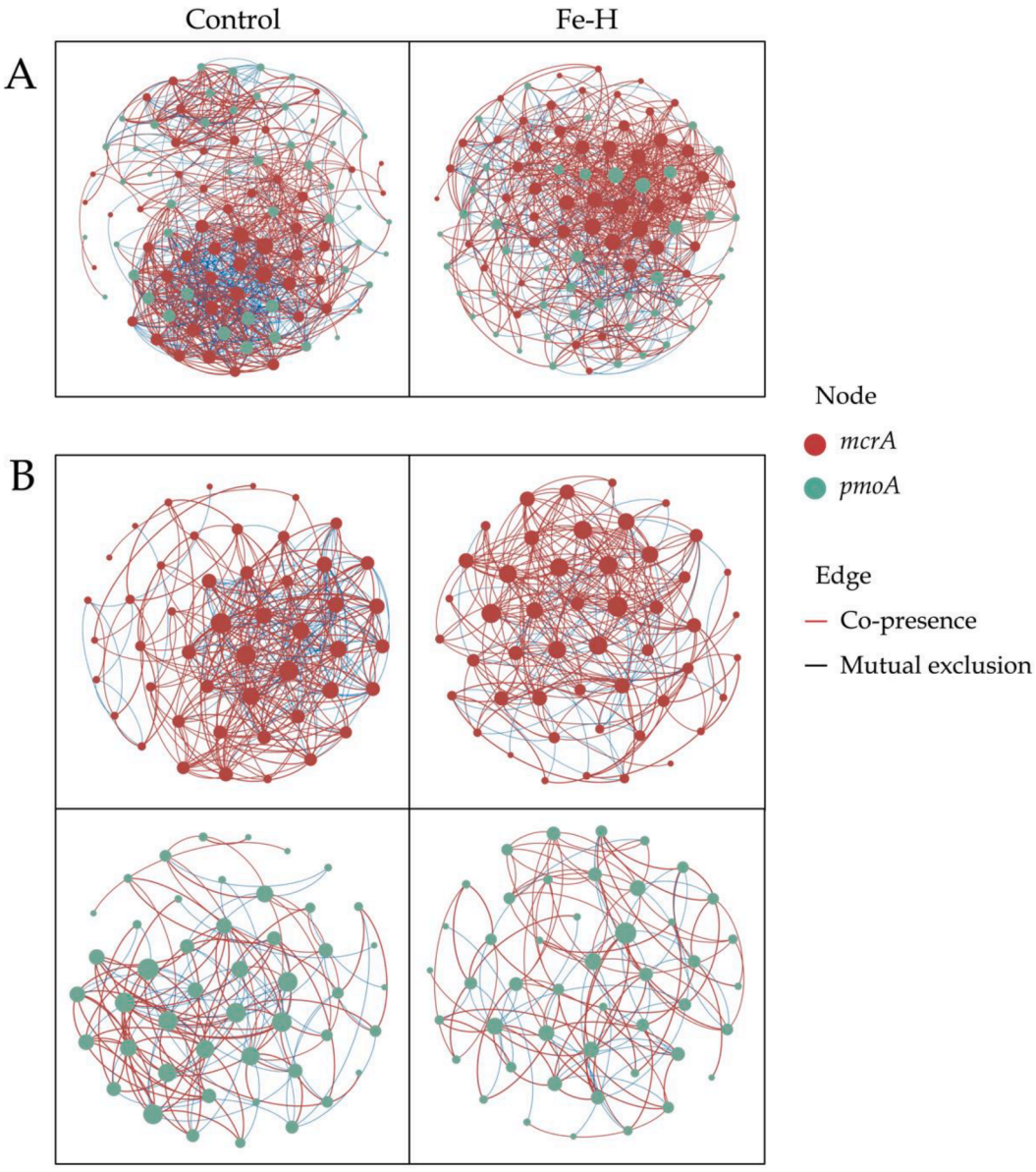

Fig. 7. Microbial co-occurrence networks of the control and Fe-H treatments. (A) Integrated microbial co-occurrence networks across methanogens and methanotrophs. Network construction is based on the proportion of OUT datasets. Nodes represent individual OTUs, and edges represent significant correlations. Network nodes indicating OTUs are depicted as spheres (red, *mcrA*; green, *pmoA*), and edges are coloured by interaction types (co-presence in red; mutual exclusion in black). The node size is proportional to the average degree of each taxon. (B) Separate microbial co-occurrence networks within methanogens and methanotrophs, respectively. Features of nodes and edges are the same as described in panel A.

resistance to salt stress (Osudar et al., 2017). In our study, Type II methanotrophs (e.g., *Methylocystis*) were more abundant and active, while Type I methanotrophs (e.g., *Methylomonas*) were relatively suppressed by Fe(III) fertiliser addition (Fig. 3b). Type II methanotrophs exhibit lower methane yields than Type I methanotrophs, a fact attributed to a serine pathway (Kalyuzhnaya et al., 2015). Han et al (2017) revealed that Type II methanotrophs are resistant to relatively low salt stress. Moreover, when the available substrate level is limited, Type II methanotrophs can alter their survival strategy (Ho et al., 2013). Importantly, Type II methanotrophs, such as *Methylocystis*, strain SB2 may contain two enzymes with low and high levels of affinity for adapting to various CH_4 concentrations, and consume ethanol and acetate for growth (Im et al., 2011). In this study, the relative abundance of *Methylocystis* was greater in the treatments than in the control. Moreover, the relative abundance of *Methylocystis* increased by 33% and 16% in Fe-M and Fe-H treatments, respectively, compared to the control in the drainage stage (Fig. 3b). Thus, the superiority of Type II methanotrophs over Type I methanotrophs at low-methane concentrations may also be a selective advantage in rice paddies, where growth is periodically restricted because of fluctuations in the methane supply (Baani and Liesack, 2008).

In contrast to methanotrophs being affected by soil salinity, methanogens can be affected by Fe(III) oxides more directly. In our study we divided methanogenic genera into two groups according to their responses to Fe(III) fertiliser application (Fig. 4a). Among the positive response genera were *Methanothrix*, whose relative abundance increased in Fe(III) fertilised treatments. Importantly, this increase can be attributed to the direct interspecies electron transfer (DIET) (Rotaru et al., 2014), and Fe(III) oxides may serve as electron conduits to stimulate DIET (Cruz Viggi et al., 2014). However, an increase in the relative abundance of *Methanothrix* indicates a decrease in other methanogenic genera that may have a stronger capacity for CH_4 production (e.g.,

Table 3
Topological parameters of the integrated microbial co-occurrence networks in the control and Fe-H treatments.

	Control	Fe-H
Nodes		
Number of nodes	97	95
Percentage of *mcrA* nodes (%)	49.48	51.58
Percentage of *pmoA* nodes (%)	50.52	48.42
Average degree	17.608	15.6
Edges		
Number of edges	854	741
Percentage of *mcrA-mcrA* edges (%)	38.52	39.00
Percentage of *pmoA-pmoA* edges (%)	16.86	17.54
Percentage of *mcrA-pmoA* edges (%)	44.61	43.45
Positive edges (%)	64.64	79.76
Negative edges (%)	35.36	20.24
Average path distance (GD)	2.367	2.167
Network		
Clustering coefficient	0.633	0.518
Network density	0.183	0.166

Table 4
Topological parameters of the separate microbial co-occurrence networks in the control and Fe-H treatment.

	Methanogens		Methanotrophs	
	Control	Fe-H	Control	Fe-H
Nodes				
Number of nodes	48	49	47	46
Average degree	13.708	11.796	6.128	5.652
Edges				
Number of edges	329	289	144	130
Percentage of positive edges (%)	66.87	83.74	63.89	70.77
Percentage of negative edges (%)	33.13	16.26	36.11	29.23
Average path distance (GD)	2.265	1.976	2.884	2.89
Network				
Clustering coefficient	0.666	0.568	0.603	0.541
Network density	0.292	0.246	0.133	0.126

Methanocella and *Methanobacterium*). *Methanocella* are hydrogenotrophic methanogens known as rice cluster I and play a key role in CH_4 production in rice soil (Lu and Conrad, 2005). Many H_2-utilising methanogens can transfer electrons to poorly crystalline Fe(III) oxide, and this can be one explanation for the inhibition of methanogenesis in Fe(III)-rich ecosystems (Bond and Lovley, 2002; van Bodegom et al., 2004). In Fig. 4b, the steeper slope of the regression line of negatively responsive genera implies that the mitigation of CH_4 emissions could be due to a decrease in the CH_4 production efficiency of the predominant methanogens caused by Fe(III) fertiliser addition. Therefore, Fe(III) fertiliser-decreased CH_4 emissions can also be achieved through the change in methanogenic community composition.

Overall, according to our results, *Methanothrix* became the most obviously changed genus in the paddy soils and grew better in Fe-rich environments. However, in this study, adding Fe(III) fertiliser decreased the CH_4 production efficiency from predominant methanogen genera (e.g. *Methanocella* and *Methanobacterium*). This finding is consistent with the results of MPPs, showing that Fe(III) amendment suppressed the soil CH_4 production capacity. On the other hand, the relative abundance of *Methylocystis* (Type II) was significantly and negatively related to CH_4 fluxes (Fig. 6b). *Methylomonas* (Type I) varied with treatments and is significantly negatively correlated to MOPs, showing that Type I methanotrophs' activity was inhibited by Fe(III) fertiliser addition.

Taken together, these results show the methanotroph community plays an important role in CH_4 oxidation. After Fe(III) fertiliser addition, Type II methanotrophs were more adaptive and active, while Type I methanotrophs were relatively suppressed.

Methanogens and methanotrophs responded to Fe(III) fertiliser addition not only at the genus level but also at the OTU level, and this response was further reflected by microbial co-occurrence networks. Network modelling allows incorporating the complex relationships among microbes into an integrated pattern (Bascompte, 2007). Therefore, we constructed a microbial co-occurrence network to evaluate the effects of Fe(III) fertilisation on paddy soils and to explore the potential relationships among specific taxa (Fig. 7). Comparing the integrated co-occurrence networks between the control and Fe-H treatments showed that Fe(III) fertiliser application reduced the network complexity contrast of the control, which contained fewer nodes and edges (Table 3). The topological features of the control, such as average degree, clustering coefficient, and network density, indicate a more connected and robust network. This result suggests that the methanogenic and methanotrophic interactomes in the control are characterized by relatively higher metabolic exchange and competition among community members, which likely increased their co-occurrence (Bissett et al., 2013; Faust and Raes, 2012). On the other hand, the average path distance in the Fe-H treatment is smaller than that in the control, which means faster communication between methanogens and methanotrophs. However, in this case, local perturbations reached the whole network quickly, possibly altering the system (Kitano, 2004; Zhou et al., 2010). Thus, our results indicate that adding Fe(III) fertiliser can decrease the co-occurrence of methanogens and methanotrophs, and methanogenic and methanotrophic communities can respond more quickly to environmental changes.

By comparing the separate methanogenic and methanotrophic co-occurrence networks between the control and Fe-H treatments, we found that the network of methanogens and methanotrophs in the Fe-H treatment contains fewer edges than that in the control. This result further proves that Fe(III) fertilisation can decrease the complexity of both methanogenic and methanotrophic networks. *Methanocella* and *Methylocystis*, belonging to methanogens and methanotrophs, respectively are the network hubs in the control, while in the Fe-H treatment, *Methanothrix* dominates the methanogenic network (Table S3). Moreover, the fewer edges in the Fe-H treatment (6.34%) compared to the control (12.76%) are mostly due to the lower proportion of mutual exclusion among methanogens. This difference might reflect eased competition among methanogens after Fe(III) fertilisation. According to Bond and Lovley (2002), methanogenesis can be inhibited because of the diversion of electrons from CH_4 production to Fe^{3+} reduction. Thus, it is possible that Fe, as a density- independent factor, competes with methanogens for electrons, and then some special methanogens may lose their competitiveness in the system.

This study attempted to build a linkage between the activity, abundance and composition of methanogens and methanotrophs and seasonal CH_4 emissions in response to Fe(III) fertiliser addition in a rice paddy in southeast China. However, although we studied the abundance and composition of methanogens and methanotrophs and further explored the relationship between the CH_4 fluxes and community composition, the interaction between methanogens and methanotrophs remains unclear. In future studies, dominant genera and specific primers of methanogens and methanotrophs should be detected after Illumina MiSeq sequencing, to further quantify the absolute abundance and make community composition analysis more convincing. Importantly, in our study, microbial co-occurrence networks were constructed to evaluate methanogens and methanotrophs' response to Fe(III) fertilisation at the OTU level. However, to explore and clarify the potential connection by analysing microbial co-occurrence networks, more data on the composition of methanogen and methanotroph communities should be collected. Moreover, regarding the connection between methanogens and methanotrophs, confirmatory experiments such as incubating dominant genera belonging to methanogenic and methanotrophic communities should be conducted to find the potential relationship between them.

5. Conclusion

This study showed that the application of Fe(III) fertiliser had no adverse effect on rice yield but significantly decreased CH_4 emissions. Applying Fe(III) fertiliser significantly decreased the abundance and activity of methanogens while increasing the populations and activity of methanotrophs. Moreover, where Fe(III) changed the composition of methanogenic archaea and methanotrophic bacteria, there was a shift from Type I methanotrophs to Type II methanotrophs in their relative abundance after Fe(III) fertiliser application. Suppression of CH_4 emissions from rice paddies was associated with the conversion between Fe^{3+} and Fe^{2+}, and soil salinity was attributed to Fe(III) fertilisation. The application of Fe(III) fertiliser mitigated CH_4 emissions by decreasing CH_4 production from predominant methanogen genera and stimulating methane oxidation potentials. Our results suggest that a less complex microbial network structure within the Fe-H treatment can be associated with additional Fe(III) fertiliser, possibly reducing competition among methanogens.

Declaration of Competing Interest

The authors declare that they have no known competing financial interests or personal relationships that could have appeared to influence the work reported in this paper.

Data availability

Data will be made available on request.

Acknowledgments

This work was supported by the Jiangsu Agriculture Science and Technology Innovation Fund (JASTIF, CX(21)3007), National Natural Science Foundation of China (NSFC, 41877093, 41771323 and 41907072), and PADA. JS and JP were funded by Grant TED2021-132627B-I00 from MCIN, AEI/10.13039/501100011033 and the European Union NextGenerationEU/PRTR.

Appendix A. Supplementary data

Supplementary data to this article can be found online at https://doi.org/10.1016/j.geoderma.2023.116375.

References

Ali, M.A., Lee, C.H., Kim, P.J., 2008. Effect of silicate fertilizer on reducing methane emission during rice cultivation. Biol. Fertil. Soils 44, 597–604. https://doi.org/10.1007/s00374-007-0243-5.

Arao, T., Kawasaki, A., Baba, K., Mori, S., Matsumoto, S., 2009. Effects of water management on cadmium and arsenic accumulation and dimethylarsinic acid concentrations in Japanese rice. Environ. Sci. Tech. 43, 9361–9367. https://doi.org/10.1021/es9022738.

Baani, M., Liesack, W., 2008. Two isozymes of particulate methane monooxygenase with different methane oxidation kinetics are found in Methylocystis sp. strain SC2. PNAS 105, 10203–10208. https://doi.org/10.1073/pnas.0702643105.

Bascompte, J., 2007. Networks in ecology. Basic Appl. Ecol. 8 https://doi.org/10.1016/j.baae.2007.06.003.

Beal, E.J., House, C.H., Orphan, V.J., 2009. Manganese- and iron-dependent marine methane oxidation. Science (80-). 325, 184–187. 10.1126/science.1169984.

Bissett, A., Brown, M.V., Siciliano, S.D., Thrall, P.H., 2013. Microbial community responses to anthropogenically induced environmental change: Towards a systems approach. Ecol. Lett. 16 https://doi.org/10.1111/ele.12109.

Blazewicz, S.J., Petersen, D.G., Waldrop, M.P., Firestone, M.K., 2012. Anaerobic oxidation of methane in tropical and boreal soils: Ecological significance in terrestrial methane cycling. J. Geophys. Res. Biogeosciences 117, 1–9. https://doi.org/10.1029/2011JG001864.

Bodegom, P.M.V., Stams, A.J.M., 1999. Effects of Alternative Electron Acceptors and Temperature on. Chemosphere 39, 167–182.

Bond, D.R., Lovley, D.R., 2002. Reduction of Fe(III) oxide by methanogens in the presence and absence of extracellular quinones. Environ. Microbiol. 4, 115–124. https://doi.org/10.1046/j.1462-2920.2002.00279.x.

Bowman, J.P., Sly, L.T., Nichols, P.D., Hayward, A.C., 1994. Erratum: Revised taxonomy of the methanotrophs: Description of Methylobacter gen. nov., emendation of Methylococcus, validation of Methylosinus and Methylocystis species, and a proposal that the family Methylococcaceae includes only the group I methanotro. Int. J. Syst. Bacteriol. 44, 375. https://doi.org/10.1099/00207713-44-2-375.

Caporaso, J.G., Kuczynski, J., Stombaugh, J., Bittinger, K., Bushman, F.D., Costello, E.K., Fierer, N., Peña, A.G., Goodrich, J.K., Gordon, J.I., Huttley, G.A., Kelley, S.T., Knights, D., Koenig, J.E., Ley, R.E., Lozupone, C.A., Mcdonald, D., Muegge, B.D., Pirrung, M., Reeder, J., Sevinsky, J.R., Turnbaugh, P.J., Walters, W.A., Widmann, J., Yatsunenko, T., Zaneveld, J., Knight, R., 2010. QIIME allows analysis of high-throughput community sequencing data. Nat. Methods 7, 335–336. https://doi.org/10.1038/nmeth.f.303.

Chen, Z., Tang, Y.T., Yao, A.J., Cao, J., Wu, Z.H., Peng, Z.R., Wang, S.Z., Xiao, S., Baker, A.J.M., Qiu, R.L., 2017. Mitigation of Cd accumulation in paddy rice (Oryza sativa L.) by Fe fertilization. Environ. Pollut. 231, 549–559. https://doi.org/10.1016/j.envpol.2017.08.055.

Costello, A.M., Lidstrom, M.E., 1999. Molecular characterization of functional and phylogenetic genes from natural populations of methanotrophs in lake sediments. Appl. Environ. Microbiol. 65, 5066–5074. https://doi.org/10.1128/aem.65.11.5066-5074.1999.

Cruz Viggi, C., Rossetti, S., Fazi, S., Paiano, P., Majone, M., Aulenta, F., 2014. Magnetite particles triggering a faster and more robust syntrophic pathway of methanogenic propionate degradation. Environ. Sci. Tech. 48, 7536–7543. https://doi.org/10.1021/es5016789.

Degelmann, D.M., Borken, W., Drake, H.L., Kolb, S., 2010. Different atmospheric methane-oxidizing communities in european beech and norway spruce soils. Appl. Environ. Microbiol. 76, 3228–3235. https://doi.org/10.1128/AEM.02730-09.

Edgar, R.C., Haas, B.J., Clemente, J.C., Quince, C., Knight, R., 2011. UCHIME improves sensitivity and speed of chimera detection. Bioinformatics 27, 2194–2200. https://doi.org/10.1093/bioinformatics/btr381.

Fan, L., Dippold, M.A., Ge, T., Wu, J., Thiel, V., Kuzyakov, Y., Dorodnikov, M., 2020. Anaerobic oxidation of methane in paddy soil: Role of electron acceptors and fertilization in mitigating CH4 fluxes. Soil Biol. Biochem. 141, 107685 https://doi.org/10.1016/j.soilbio.2019.107685.

Fan, L., Schneider, D., Dippold, M.A., Poehlein, A., Wu, W., Gui, H., Ge, T., Wu, J., Thiel, V., Kuzyakov, Y., Dorodnikov, M., 2021. Active metabolic pathways of anaerobic methane oxidation in paddy soils. Soil Biol. Biochem. 156, 108215 https://doi.org/10.1016/j.soilbio.2021.108215.

Faust, K., Raes, J., 2012. Microbial interactions: From networks to models. Nat. Rev. Microbiol. 10, 538–550. https://doi.org/10.1038/nrmicro2832.

Faust, K., Raes, J., 2016. CoNet app: Inference of biological association networks using Cytoscape [version 1; referees: 2 approved with reservations]. F1000Res. 5, 1–17. https://doi.org/10.12688/F1000RESEARCH.9050.1.

Fredrickson, J.K., Gorby, Y.A., 1996. Environmental processes mediated by iron-reducing bacteria. Curr. Opin. Biotechnol. 7, 287–294. https://doi.org/10.1016/S0958-1669(96)80032-2.

Gao, D., Sheng, R., Whiteley, A.S., Moreira-Grez, B., Qin, H., Zhang, W., Zhan, Y., Wei, W., 2020. Effect of phosphorus amendments on rice rhizospheric methanogens and methanotrophs in a phosphorus deficient soil. Geoderma 368, 114312. https://doi.org/10.1016/j.geoderma.2020.114312.

Gross, K., 2008. Positive interactions among competitors can produce species-rich communities. Ecol. Lett. 11, 929–936. https://doi.org/10.1111/j.1461-0248.2008.01204.x.

Gwon, H.S., Khan, M.I., Alam, M.A., Das, S., Kim, P.J., 2018. Environmental risk assessment of steel-making slags and the potential use of LD slag in mitigating methane emissions and the grain arsenic level in rice (Oryza sativa L.). J. Hazard. Mater. 353, 236–243. https://doi.org/10.1016/j.jhazmat.2018.04.023.

Han, D., Link, H., Liesack, W., 2017. Response of Methylocystis sp. strain SC2 to salt stress: Physiology, global transcriptome, and amino acid profiles. Appl. Environ. Microbiol. 83 https://doi.org/10.1128/AEM.00866-17.

Hanson, R.S., Hanson, T.E., 1996. Methanotrophic bacteria. Microbiol. Rev. 60, 439–471. https://doi.org/10.1128/mmbr.60.2.439-471.1996.

He, W., Shohag, M.J.I., Wei, Y., Feng, Y., Yang, X., 2013. Iron concentration, bioavailability, and nutritional quality of polished rice affected by different forms of foliar iron fertilizer. Food Chem. 141, 4122–4126. https://doi.org/10.1016/j.foodchem.2013.07.005.

Heyer, J., Galschenko, V.F., Dunfield, P.F., 2002. Molecular phylogeny of type II methane-oxidizing bacteria isolated from various environments. Microbiology 148, 2831–2846. https://doi.org/10.1099/00221287-148-9-2831.

Ho, A., Kerckhof, F.M., Luke, C., Reim, A., Krause, S., Boon, N., Bodelier, P.L.E., 2013. Conceptualizing functional traits and ecological characteristics of methane-oxidizing bacteria as life strategies. Environ. Microbiol. Rep. 10.1111/j.1758-2229.2012.00370.x.

Ho, A., Lüke, C., Frenzel, P., 2011. Recovery of methanotrophs from disturbance: Population dynamics, evenness and functioning. ISME J. 5, 750–758. https://doi.org/10.1038/ismej.2010.163.

Holmes, A.J., Costello, A., Lidstrom, M.E., Murrell, J.C., 1995. Evidence that participate methane monooxygenase and ammonia monooxygenase may be evolutionarily related. FEMS Microbiol. Lett. 132, 203–208. https://doi.org/10.1016/0378-1097(95)00311-R.

Im, J., Lee, S.W., Yoon, S., Dispirito, A.A., Semrau, J.D., 2011. Characterization of a novel facultative Methylocystis species capable of growth on methane, acetate and ethanol. Environ. Microbiol. Rep. 3, 174–181. https://doi.org/10.1111/j.1758-2229.2010.00204.x.

IPCC, 2013. Climate Change 2013-The Physical Science Basis. Contribution of Working Group I to the Fifth Assessment Report of the Intergovernmental Panel on Climate Change. Cambridge University Press, Cambridge, New York.
Kalyuzhnaya, M.G., Puri, A.W., Lidstrom, M.E., 2015. Metabolic engineering in methanotrophic bacteria. Metab. Eng. 29, 142–152. https://doi.org/10.1016/j.ymben.2015.03.010.
Karimi, B., Maron, P.A., Chemidlin-Prevost Boure, N., Bernard, N., Gilbert, D., Ranjard, L., 2017. Microbial diversity and ecological networks as indicators of environmental quality. Environ. Chem. Lett. 15, 265–281. https://doi.org/10.1007/s10311-017-0614-6.
Kaupper, T., Mendes, L.W., Lee, H.J., Mo, Y., Poehlein, A., Jia, Z., Horn, M.A., Ho, A., 2021. When the going gets tough: Emergence of a complex methane-driven interaction network during recovery from desiccation-rewetting. Soil Biol. Biochem. 153, 108109 https://doi.org/10.1016/j.soilbio.2020.108109.
Kim, G.W., Ho, A., Kim, P.J., Kim, S.Y., 2016. Stimulation of methane oxidation potential and effects on vegetation growth by bottom ash addition in a landfill final evapotranspiration cover. Waste Manage. 55, 306–312. https://doi.org/10.1016/j.wasman.2016.03.058.
Kitano, H., 2004. Biological robustness. Nat. Rev. Genet. https://doi.org/10.1038/nrg1471.
Kong, D., Li, S., Jin, Y., Wu, S., Chen, J., Hu, T., Wang, H., Liu, S., Zou, J., 2019. Linking methane emissions to methanogenic and methanotrophic communities under different fertilization strategies in rice paddies. Geoderma 347, 233–243. https://doi.org/10.1016/j.geoderma.2019.04.008.
Li, S., Song, L., Gao, X., Jin, Y., Liu, S., Shen, Q., Zou, J., 2017. Microbial abundances predict methane and nitrous oxide fluxes from a windrow composting system. Front. Microbiol. 8 https://doi.org/10.3389/fmicb.2017.00409.
Lovley, D.R., 1987. Organic matter mineralization with the reduction of ferric iron: A review. Geomicrobiol. J. 5, 375–399. https://doi.org/10.1080/01490458709385975.
Lovley, D.R., Phillips, E.J.P., 1987. Competitive Mechanisms for Inhibition of Sulfate Reduction and Methane Production in the Zone of Ferric Iron Reduction in Sediments. Appl. Environ. Microbiol. 53, 2636–2641. https://doi.org/10.1128/aem.53.11.2636-2641.1987.
Lu, Y., Conrad, R., 2005. In situ stable isotope probing of methanogenic Archaea in the rice rhizosphere. Science (80-) 309, 1088–1090. https://doi.org/10.1126/science.1113435.
Osudar, R., Klings, K.W., Wagner, D., Bussmann, I., 2017. Effect of salinity on microbial methane oxidation in freshwater and marine environments. Aquat. Microb. Ecol. 80, 181–192. https://doi.org/10.3354/ame01845.
Pereyra, L.P., Hiibel, S.R., Prieto Riquelme, M.V., Reardon, K.F., Pruden, A., 2010. Detection and quantification of functional genes of cellulosedegrading, fermentative, and sulfate-reducing bacteria and methanogenic archaea. Appl. Environ. Microbiol. 76, 2192–2202. https://doi.org/10.1128/AEM.01285-09.
Qin, Y., Liu, S., Guo, Y., Liu, Q., Zou, J., 2010. Methane and nitrous oxide emissions from organic and conventional rice cropping systems in Southeast China. Biol. Fertil. Soils 46, 825–834. https://doi.org/10.1007/s00374-010-0493-5.
Reumer, M., Harnisz, M., Lee, H.J., Reim, A., Grunert, O., Putkinen, A., Fritze, H., Bodelier, P.L.E., Ho, A., 2018. Impact of peat mining and restoration on methane turnover potential and methane-cycling microorganisms in a northern bog. Appl. Environ. Microbiol. 84 https://doi.org/10.1128/AEM.02218-17.
Rotaru, A.E., Shrestha, P.M., Liu, F., Shrestha, M., Shrestha, D., Embree, M., Zengler, K., Wardman, C., Nevin, K.P., Lovley, D.R., 2014. A new model for electron flow during anaerobic digestion: Direct interspecies electron transfer to Methanosaeta for the reduction of carbon dioxide to methane. Energy Environ. Sci. 7, 408–415. https://doi.org/10.1039/c3ee42189a.
Singh, A., Singh, R.S., Upadhyay, S.N., Joshi, C.G., Tripathi, A.K., Dubey, S.K., 2012. Community structure of methanogenic archaea and methane production associated with compost-treated tropical rice-field soil. FEMS Microbiol. Ecol. 82, 118–134. https://doi.org/10.1111/j.1574-6941.2012.01411.x.
Sonoki, T., Furukawa, T., Jindo, K., Suto, K., Aoyama, M., Sánchez-Monedero, M.Á., 2013. Influence of biochar addition on methane metabolism during thermophilic phase of composting. J. Basic Microbiol. 53, 617–621. https://doi.org/10.1002/jobm.201200096.
Steinberg, L.M., Regan, J.M., 2008. Phylogenetic comparison of the methanogenic communities from an acidic, oligotrophic fen and an anaerobic digester treating municipal wastewater sludge. Appl. Environ. Microbiol. 74, 6663–6671. https://doi.org/10.1128/AEM.00553-08.
Stookey, L.L., 1970. Ferrozine–a new spectrophotometric reagent for iron. Anal. Chem. 42 (7), 779–781.
Sun, H., Zhou, S., Fu, Z., Chen, G., Zou, G., Song, X., 2016. A two-year field measurement of methane and nitrous oxide fluxes from rice paddies under contrasting climate conditions. Sci. Rep. 6, 1–11. https://doi.org/10.1038/srep28255.
Tokida, T., Fumoto, T., Cheng, W., Matsunami, T., Adachi, M., Katayanagi, N., Matsushima, M., Okawara, Y., Nakamura, H., Okada, M., Sameshima, R., Hasegawa, T., 2010. Effects of free-air CO2 enrichment (FACE) and soil warming on CH4 emission from a rice paddy field: Impact assessment and stoichiometric evaluation. Biogeosciences 7, 2639–2653. https://doi.org/10.5194/bg-7-2639-2010.
Van Bodegom, P.M., Scholten, J.C.M., Stams, A.J.M., 2004. Direct inhibition of methanogenesis by ferric iron. FEMS Microbiol. Ecol. 49, 261–268. https://doi.org/10.1016/j.femsec.2004.03.017.
Wang, C., Jin, Y., Ji, C., Zhang, N., Song, M., Kong, D., Liu, S., Zhang, X., Liu, X., Zou, J., Li, S., Pan, G., 2018. An additive effect of elevated atmospheric CO2 and rising temperature on methane emissions related to methanogenic community in rice paddies. Agr. Ecosyst. Environ. 257, 165–174. https://doi.org/10.1016/j.agee.2018.02.003.
Wasmund, K., Kurtböke, D.I., Burns, K.A., Bourne, D.G., 2009. Microbial diversity in sediments associated with a shallow methane seep in the tropical Timor Sea of Australia reveals a novel aerobic methanotroph diversity. FEMS Microbiol. Ecol. 68, 142–151. https://doi.org/10.1111/j.1574-6941.2009.00667.x.
Weber, K.A., Achenbach, L.A., Coates, J.D., 2006. Microorganisms pumping iron: Anaerobic microbial iron oxidation and reduction. Nat. Rev. Microbiol. 4, 752–764. https://doi.org/10.1038/nrmicro1490.
Xu, B., Wang, F., Zhang, Q., Lan, Q., Liu, C., Guo, X., Cai, Q., Chen, Y., Wang, G., Ding, J., 2018. Influence of iron plaque on the uptake and accumulation of chromium by rice (Oryza sativa L.) seedlings: Insights from hydroponic and soil cultivation. Ecotoxicol. Environ. Saf. 162, 51–58. https://doi.org/10.1016/j.ecoenv.2018.06.063.
Yang, S., Liebner, S., Alawi, M., Ebenhöh, O., Wagner, D., 2014. Taxonomic database and cut-off value for processing mcrA gene 454 pyrosequencing data by MOTHUR. J. Microbiol. Methods 103, 3–5. https://doi.org/10.1016/j.mimet.2014.05.006.
Yu, K., Fang, X., Zhang, Y., Miao, Y., Liu, S., Zou, J., 2021. Low greenhouse gases emissions associated with high nitrogen use efficiency under optimized fertilization regimes in double-rice cropping systems. Appl. Soil Ecol. 160, 103846 https://doi.org/10.1016/j.apsoil.2020.103846.
Zhang, J., Dong, H., Liu, D., Fischer, T.B., Wang, S., Huang, L., 2012. Microbial reduction of Fe(III) in illite-smectite minerals by methanogen Methanosarcina mazei. Chem. Geol. 292–293, 35–44. https://doi.org/10.1016/j.chemgeo.2011.11.003.
Zhou, J., Deng, Y., Luo, F., He, Z., Tu, Q., Zhi, X., 2010. Functional molecular ecological networks. MBio 1. https://doi.org/10.1128/mBio.00169-10.
Zhou, P., Pan, G.X., Zhang X.H., Song, X.Y., Li, L., 2009. An approach of C sequestration and metigation inspired by ferric oxide from paddy soil. Journal of Agro-Environment Science 28, 2590-2595 (in Chinese with English Abstract). doi: 10.3321/j.issn:1672-2043.2009.12.024.
Zhou, G., Gao, S., Xu, C., Dou, F., Shimizu, K. yoshi, Cao, W., 2020. Rational utilization of leguminous green manure to mitigate methane emissions by influencing methanogenic and methanotrophic communities. Geoderma 361, 114071. https://doi.org/10.1016/j.geoderma.2019.114071.
Zou, J., Huang, Y., Xi, Z., 2004. Carbon Dioxide, Methane, and Nitrous Oxide Emissions from. Advances 21, 691–698.
Zou, J., Huang, Y., Jiang, J., Zheng, X., Sass, R.L., 2005. A 3-year field measurement of methane and nitrous oxide emissions from rice paddies in China: Effects of water regime, crop residue, and fertilizer application. Global Biogeochem. Cycles 19, 1–9. https://doi.org/10.1029/2004GB002401.
Zou, J., Liu, S., Qin, Y., Pan, G., Zhu, D., 2009. Sewage irrigation increased methane and nitrous oxide emissions from rice paddies in southeast China. Agr. Ecosyst. Environ. 129, 516–522. https://doi.org/10.1016/j.agee.2008.11.006.